

No-three-in-line sets on the checkerboard grid

Thomas Prellberg

School of Mathematical Sciences
Queen Mary University of London
United Kingdom

t.prellberg@qmul.ac.uk

May 12, 2026

Abstract

The classical no-three-in-line problem asks for the largest number $D(n)$ of points that can be chosen from an $n \times n$ grid with no three collinear. It remains open whether the elementary upper bound $2n$ is always attainable. We study a checkerboard-restricted variant in which all chosen points must lie in one fixed parity class of the colouring by $x + y \pmod{2}$. If $D_{\text{mono}}(n)$ denotes the corresponding single-parity optimum, then the slope- ± 1 diagonals already give the elementary bound $D_{\text{mono}}(n) \leq 2n - 2$.

The main object of the paper is a four-direction linear-programming relaxation on a fixed parity class, using rows, columns, and the two diagonal families of slopes ± 1 . For the ordinary square-grid problem this relaxation gives the trivial bound. On the checkerboard it gives substantially tighter finite bounds in the computed range. For $2 \leq n \leq 16$ its floor agrees with the exact single-parity optimum except at four side lengths, where the gap is one. After symmetry reduction, the dual relaxation has three one-dimensional reduced forms, according to the parity of n and the chosen colour class; their computed optimizers display structured piecewise-profile patterns.

The central rigorous result is a continuum dual certificate for the formal continuum problem associated with the scaled symmetry-reduced odd-fat case. We construct explicit nonnegative functions A and B satisfying the continuum obstacle inequalities and having objective value α , where

$$401\alpha^3 - 1744\alpha^2 + 2240\alpha - 768 = 0$$

and α is the middle real root. This proves the upper bound $\Lambda_{\text{fat}} \leq \alpha$ for the odd-fat continuum relaxation. Finite LP computations are consistent with α as a limiting slope, and the exact small- n data suggest, more speculatively, that the true checkerboard optimum may track the same scale. We state the corresponding limiting interpretation for the discrete LP as a conjecture, and formulate the analogous statement for $D_{\text{mono}}(n)$ as a stronger conjecture.

1 Introduction

The no-three-in-line problem, introduced by Dudeney in recreational form and later developed in the combinatorics literature, asks for the maximum number $D(n)$ of points that can be selected from the $n \times n$ integer grid so that no three lie on a common line [12, 21, 22]. The pigeonhole principle gives the elementary upper bound $D(n) \leq 2n$. The problem of attaining this bound has been studied extensively. See, for example, [1, 3, 16, 17, 23, 24, 30] and the broader accounts in [6, 14].

Several neighbouring variants are close enough to be worth separating from the present one. Finite-torus and other modular versions ask for collinearity modulo a finite abelian group [18, 26,

32]; permutation or transversal versions study related collinearity restrictions in permutation-like sets [10, 11]; and higher-dimensional grid versions have also been studied [29]. Other nearby problems concern minimum or extensible no-three-in-line sets [2, 9, 27], as well as no- $(k + 1)$ -in-line generalisations [25]. For arbitrary input point sets, the general-position subset selection problem is studied both combinatorially and algorithmically [4, 13, 19, 20, 28].

This paper studies a parity-restricted version of the same problem. Write $[n]_0 := \{0, 1, \dots, n - 1\}$ and colour $[n]_0^2$ by the parity of $x + y$. The two colour classes C_0 and C_1 are defined formally in Definition 1. For a fixed colour $\varepsilon \in \{0, 1\}$, let $D_{\text{mono}}(n, \varepsilon)$ be the largest size of a no-three-in-line set contained in C_ε , and put

$$D_{\text{mono}}(n) = \max_{\varepsilon \in \{0, 1\}} D_{\text{mono}}(n, \varepsilon).$$

When $n = 2m + 1$ is odd, the two colour classes have sizes $2m^2 + 2m + 1$ and $2m^2 + 2m$. We call the larger one the *fat* class and the smaller one the *thin* class. For even n the two classes have equal size. The adjective “monochromatic” is used here only with respect to this fixed checkerboard colouring: a feasible set is required to lie in one of the two parity classes C_0, C_1 . This is different from colouring the whole grid so that every colour class has the no-three-in-line property, as in Wood’s grid-colouring problem [33], and from graph-theoretic position-set colourings [8]. The author has not found a prior published treatment of the present square-grid parity-class maximisation problem. The neighbouring colouring and general-position references above provide context, but no result from them is used in the proof of the continuum certificate below.

The checkerboard restriction is motivated by a simple obstruction to extending maximal configurations. Suppose that a $2n$ -point no-three-in-line set on an $n \times n$ grid is dilated by a factor of two and placed in the $2n \times 2n$ grid. Since a $2n$ -point configuration uses exactly two points in every row and every column of the original grid, the dilated configuration already saturates all even rows and all even columns of the larger grid. Any additional points in a putative completion to a $4n$ -point configuration would therefore have to lie in odd rows and odd columns. Thus all added points would lie in a single checkerboard colour class. Single-parity no-three-in-line sets are therefore one natural finite-grid test case for possible obstructions to such completions.

There is also an immediate capacity obstruction. In one checkerboard class, every diagonal of slope $+1$ and every diagonal of slope -1 is monochromatic. Each such diagonal can therefore contain at most two selected points, and counting the capacity of one diagonal family gives

$$D_{\text{mono}}(n) \leq 2n - 2.$$

Section 3 proves this bound. A boundary-forcing mechanism suggests, but does not prove, the sharper inequality $D_{\text{mono}}(n) \leq 2n - 4$ for $n \geq 6$. Appendix A records the heuristic local forcing mechanism behind this expectation.

The main tool in the paper is the four-direction linear-programming relaxation $L_{\text{mono}}(n, \varepsilon)$. This relaxation replaces the integral choice of points in C_ε by a nonnegative fractional mass assignment and keeps the capacity-two constraints on rows, columns, and the two diagonal families of slopes ± 1 . Hence

$$D_{\text{mono}}(n, \varepsilon) \leq L_{\text{mono}}(n, \varepsilon).$$

For the ordinary square-grid no-three-in-line problem, the analogous relaxation gives the trivial bound $2n$. On the checkerboard, however, the same four directions become much more informative in the computations reported here. Separate exact search for $2 \leq n \leq 16$ shows that the floor of the LP optimum agrees with $D_{\text{mono}}(n, \varepsilon)$ except in four side lengths, where the gap is one.

The dual form of this LP is particularly useful. A dual solution assigns nonnegative weights to rows, columns, and diagonals, with the requirement that every point of the chosen colour class

is covered by total weight at least one. Any such weighting is an explicit upper-bound certificate. By averaging over the symmetries preserving the chosen colour class, the dual problem reduces to one-dimensional line-weight profiles. The three cases are odd side length with the fat class, odd side length with the thin class, and even side length. The computed reduced LP optimizers display a stable piecewise-profile pattern and point numerically to a common linear scale

$$L_{\text{mono}}(n, \varepsilon) \approx \alpha n, \quad \alpha \approx 1.5768.$$

At the small sizes where exact search is feasible, the true values $D_{\text{mono}}(n, \varepsilon)$ are consistent with the same scale.

The main rigorous result of the paper is an exact continuum upper-bound certificate at this constant in the cleanest of the three symmetry types, namely the odd-fat case. A formal scaling of the reduced variables leads to a continuum obstacle problem. One seeks nonnegative functions A, B on $[0, 1]$ minimizing

$$4 \int_0^1 (A(t) + B(t)) dt$$

subject to

$$A(x) + A(1 - y) + B(x + y) + B(x - y) \geq 1$$

on the triangle

$$T = \{(x, y) : 0 \leq y \leq x, x + y \leq 1\}.$$

Theorem 1, proved in Subsection 4.2, constructs explicit piecewise quadratic and linear functions A and B satisfying these inequalities. Their objective value is the middle real root α of

$$401\alpha^3 - 1744\alpha^2 + 2240\alpha - 768 = 0.$$

The obstacle inequality is verified by an exact algebraic Bernstein-basis certificate over a finite subdivision of the continuum domain.

The construction proves the rigorous upper bound $\Lambda_{\text{fat}} \leq \alpha$ for the odd-fat continuum relaxation. It does not by itself prove any discrete asymptotic theorem. The finite LP data support the conjecture that $L_{\text{mono}}(n, \varepsilon)/n$ tends to α in all three symmetry types. The exact small- n data suggest the same scale for the original monochromatic no-three-in-line problem. We formulate these discrete asymptotic statements as conjectures following the reduced LP evidence.

The paper is organised as follows. Section 2 fixes the basic notation and parity terminology. Section 3 gives the elementary diagonal bound. Section 4 introduces the four-direction LP relaxation and its dual certificate interpretation. Proposition 3 records the three symmetry-reduced dual programs in Subsection 4.1. Subsection 4.2 states and verifies the odd-fat continuum certificate. Appendix A records the boundary-forcing heuristic, Appendix B records finite profile-curvature data, and Appendix C gives the active-patch ansatz calculation behind the continuum certificate. A final reproducibility note describes the companion certificate package.

2 Definitions and notation

Definition 1 (Checkerboard colour classes). Let $n \in \mathbb{N}$ and let $G_n := [n]_0^2 \subset \mathbb{Z}^2$. For $\varepsilon \in \{0, 1\}$ define the parity (checkerboard) classes

$$C_\varepsilon := \{(x, y) \in G_n : x + y \equiv \varepsilon \pmod{2}\}.$$

We will refer to C_0 and C_1 as the two *colours*. The labels “black” and “white” are immaterial.

Definition 2 (No-three-in-line (NTIL) and monochromatic optima). A finite set $S \subset \mathbb{Z}^2$ is *no-three-in-line* (NTIL) if no three points of S are collinear. For fixed $n \in \mathbb{N}$ and $\varepsilon \in \{0, 1\}$, define

$$D_{\text{mono}}(n, \varepsilon) := \max\{|S| : S \subseteq C_\varepsilon \text{ is NTIL}\}.$$

We then set

$$D_{\text{mono}}(n) = \max_{\varepsilon \in \{0, 1\}} D_{\text{mono}}(n, \varepsilon).$$

The term “monochromatic” in Definition 2 is therefore shorthand for “contained in one prescribed parity class of the fixed checkerboard colouring”. It should not be read as a statement about arbitrary colourings of the grid or as a graph-colouring condition.

For $c \in \mathbb{Z}$ we write

$$D_c^+ := \{(x, y) \in G_n : x - y = c\}, \quad D_c^- := \{(x, y) \in G_n : x + y = c\},$$

for the diagonals of slope $+1$ and -1 respectively (intersected with the grid).

Lemma 1 (Slope- ± 1 diagonals are monochromatic). *Each diagonal D_c^+ and D_c^- lies entirely in a single parity class.*

Proof. Along D_c^+ one has $x - y = c$, so $x + y \equiv 2y + c \equiv c \pmod{2}$. Along D_c^- one has $x + y = c$ identically. In either case the parity of $x + y$ is constant along the diagonal. \square

Remark 1 (Fat and thin classes). For odd $n = 2m + 1$, one colour class has $2m^2 + 2m + 1 = (n^2 + 1)/2$ points and the other has $2m^2 + 2m = (n^2 - 1)/2$ points. We call the larger class the *fat* class and the smaller one the *thin* class. The labels C_0 and C_1 depend on which corner colour is chosen. For even n the two colour classes have the same cardinality, so this terminology is unnecessary.

3 Elementary diagonal bound

The first obstruction comes from Lemma 1. Inside a fixed colour class, every diagonal of slope $+1$ and every diagonal of slope -1 is monochromatic.

Proposition 1 (Diagonal capacity). *Fix $n \geq 2$ and $\varepsilon \in \{0, 1\}$. The parity class C_ε has total capacity $2n - 2$ on the diagonals of slope $+1$. Consequently every monochromatic NTIL set $S \subseteq C_\varepsilon$ satisfies*

$$|S| \leq 2n - 2.$$

Proof. Along a diagonal of slope $+1$, the parity of $x + y$ is constant. If C_ε meets n such diagonals, then two are singleton diagonals and the remaining $n - 2$ have NTIL capacity two, giving total capacity $1 + 1 + 2(n - 2) = 2n - 2$. If C_ε meets $n - 1$ such diagonals, each has capacity two, again giving $2n - 2$. \square

Remark 2 (Boundary forcing heuristic). For $n \geq 6$, the local saturation pattern behind Proposition 1 appears to rule out both $2n - 2$ and $2n - 3$ monochromatic points, although the argument recorded here is not a complete proof. This suggests the sharpened bound

$$D_{\text{mono}}(n) \leq 2n - 4 \quad (n \geq 6).$$

Appendix A records the forcing mechanism as motivation for this expected sharpening. The LP and continuum arguments below are independent of this heuristic.

Remark 3 (The exceptional case $n = 5$). The case $n = 5$ is exceptional. The monochromatic set

$$\{(0, 1), (0, 3), (1, 0), (1, 4), (3, 0), (3, 4), (4, 1), (4, 3)\}$$

has $8 = 2n - 2$ points and is NTIL.

4 A four-direction linear programming bound

We next replace the exact monochromatic optimisation problem by a four-direction fractional relaxation. In addition to the diagonal families D_c^+ and D_c^- , let

$$H_y := \{(x, y) \in G_n : x \in [n]_0\}, \quad V_x := \{(x, y) \in G_n : y \in [n]_0\},$$

denote the horizontal and vertical grid lines.

The usual exact integer-programming formulation for NTIL or general-position subset selection may include one constraint for every grid line containing at least three available points, or equivalently for every collinear triple [19, 30]. The relaxation below is deliberately weaker: it keeps only the four line families 0 , ∞ , and ± 1 . Its usefulness comes from the checkerboard restriction and from the explicit dual certificates, not from any general claim that four directions control the full no-three-in-line problem.

Every monochromatic NTIL set satisfies all of the line-capacity constraints below, so these four line families still produce a genuine relaxation of the combinatorial problem. Instead of choosing points integrally, we assign a nonnegative variable z_p to each lattice point $p \in C_\varepsilon$. One should think of z_p as a fractional amount of mass placed at p . We then enforce the capacity-two constraints on rows, columns, and diagonals of slope ± 1 . For fixed n and ε , let $L_{\text{mono}}(n, \varepsilon)$ be the optimum of

$$\max \sum_{p \in C_\varepsilon} z_p$$

subject to

$$\begin{aligned} \sum_{p \in H_y \cap C_\varepsilon} z_p &\leq 2 && (y \in [n]_0), \\ \sum_{p \in V_x \cap C_\varepsilon} z_p &\leq 2 && (x \in [n]_0), \\ \sum_{p \in D_c^+ \cap C_\varepsilon} z_p &\leq 2 && (c \in \mathbb{Z}), \\ \sum_{p \in D_c^- \cap C_\varepsilon} z_p &\leq 2 && (c \in \mathbb{Z}), \end{aligned}$$

and $z_p \geq 0$ for all $p \in C_\varepsilon$.

Proposition 2. *For every $n \geq 2$ and $\varepsilon \in \{0, 1\}$,*

$$D_{\text{mono}}(n, \varepsilon) \leq L_{\text{mono}}(n, \varepsilon).$$

Moreover, by linear programming duality,

$$L_{\text{mono}}(n, \varepsilon) = \min 2 \left(\sum_{y=0}^{n-1} h_y + \sum_{x=0}^{n-1} v_x + \sum_{c=-(n-1)}^{n-1} \lambda_c^+ + \sum_{c=0}^{2n-2} \lambda_c^- \right),$$

where the minimum is taken over nonnegative weights

$$h_y, v_x \geq 0, \quad \lambda_c^+ \geq 0 \quad (-(n-1) \leq c \leq n-1), \quad \lambda_c^- \geq 0 \quad (0 \leq c \leq 2n-2)$$

satisfying

$$h_y + v_x + \lambda_{x-y}^+ + \lambda_{x+y}^- \geq 1 \quad \text{for every } (x, y) \in C_\varepsilon.$$

Proof. If $S \subseteq C_\varepsilon$ is NTIL, then its characteristic vector is feasible for the primal linear program, because every horizontal line, vertical line, and diagonal of slope ± 1 contains at most two points of S . Hence $|S| \leq L_{\text{mono}}(n, \varepsilon)$, and maximising over all such sets gives $D_{\text{mono}}(n, \varepsilon) \leq L_{\text{mono}}(n, \varepsilon)$. The displayed dual formulation is the standard dual of the primal packing problem; see, for example, Schrijver [31]. The relevant diagonal offsets are $-(n-1), \dots, n-1$ for D_c^+ and $0, \dots, 2n-2$ for D_c^- , because all other diagonals miss the grid. Thus the dual is a finite linear program. \square

The dual variables have a simple interpretation. The weights h_y, v_x, λ_c^+ , and λ_c^- are assigned to rows, columns, and diagonals, and the constraint

$$h_y + v_x + \lambda_{x-y}^+ + \lambda_{x+y}^- \geq 1$$

means that every admissible lattice point $(x, y) \in C_\varepsilon$ is covered with total weight at least 1. Any feasible choice of these dual weights is therefore an *upper-bound certificate*, because its objective value is automatically an upper bound for $L_{\text{mono}}(n, \varepsilon)$, and hence for $D_{\text{mono}}(n, \varepsilon)$ as well.

This line-cover language is close to, but distinct from, LP/ILP viewpoints in broader General Position Subset Selection work. Cao formulated a related line-cover dual problem in his thesis, and Froese, Kanj, Nichterlein and Niedermeier discuss an ILP formulation for General Position Subset Selection that is dual to an ILP for Point Line Cover [7, 19]. The exact rows/columns/slope- ± 1 checkerboard relaxation and the continuum certificate below are specific to the present problem; the novelty claimed here is not LP duality in the abstract.

The quantity $L_{\text{mono}}(n, \varepsilon)$ ignores all slopes other than 0, ∞ and ± 1 . For the classical square-grid no-three-in-line problem, the analogous four-direction relaxation collapses to the trivial upper bound $2n$. Indeed, the constant fractional assignment $z_{x,y} = 2/n$ is primal feasible, while the dual solution assigning weight $1/2$ to each row and each column, and weight 0 to the two diagonal families, has the same value. For the checkerboard problem, however, the same relaxation is substantially more informative in the computed range. The exact values $D_{\text{mono}}(n, \varepsilon)$ reported below were obtained by direct exhaustive search for $2 \leq n \leq 16$, while the LP values were obtained by solving the corresponding primal linear programs. These finite computations are evidence only; they are not used in the proof of the continuum certificate.

n	$L_{\text{mono}}(n, 0)$	$D_{\text{mono}}(n, 0)$	$L_{\text{mono}}(n, 1)$	$D_{\text{mono}}(n, 1)$
2	2.000	2	2.000	2
3	4.000	4	4.000	4
4	6.000	6	6.000	6
5	7.200	7	8.000	8
6	9.000	8	9.000	8
7	10.667	10	10.667	10
8	12.333	12	12.333	12
9	14.133	14	13.714	13
10	15.556	15	15.556	15
11	17.120	16	17.000	16
12	18.750	18	18.750	18
13	20.267	20	20.364	20
14	22.000	21	22.000	21
15	23.478	23	23.500	23
16	25.091	24	25.091	24

Table 1: Comparison of the four-direction LP bound $L_{\text{mono}}(n, \varepsilon)$ with the exact checkerboard NTIL maxima $D_{\text{mono}}(n, \varepsilon)$ for $2 \leq n \leq 16$.

In the computed range $2 \leq n \leq 16$, using the exact LP optima rather than the rounded

values displayed in Table 1, we find

$$\lfloor L_{\text{mono}}(n, \varepsilon) \rfloor = D_{\text{mono}}(n, \varepsilon)$$

for all cases other than $n \in \{6, 11, 14, 16\}$. At those four side lengths, both parity classes satisfy

$$\lfloor L_{\text{mono}}(n, \varepsilon) \rfloor = D_{\text{mono}}(n, \varepsilon) + 1.$$

Thus, in the computed range, the four-direction LP is close to the exact checkerboard values. The remaining LP gap shows that these four line families alone do not determine the exact NTIL optimum in every case.

4.1 Three symmetry-reduced dual LPs

The generic dual in Proposition 2 hides an important distinction. There are three symmetry types. For odd side length the full dihedral symmetry preserves each colour class, whereas for even side length a 90° rotation swaps the two colours and therefore is unavailable in a fixed one-colour optimisation problem. The following proposition records the resulting reduced dual programs. The variables in these programs are orbit-averaged versions of the row, column, and diagonal weights in Proposition 2.

The reduction is an averaging argument in the dual. Since the objective and constraints are invariant under the colour-preserving symmetries, an optimal dual weighting may be chosen constant on line orbits. The work is to list these orbits and their objective coefficients in the three parity cases.

Proposition 3 (Symmetry-reduced dual programs). *The four-direction dual LP may be reduced as follows.*

1. **Odd side length, fat class.** Let $n = 2m + 1$ and consider the fat class C_0 . Then

$$L_{\text{mono}}(2m + 1, 0) = \min \Phi_m^{\text{fat}}(a, b),$$

where

$$\Phi_m^{\text{fat}}(a, b) := 8 \sum_{i=0}^{m-1} (a_i + b_i) + 4(a_m + b_m),$$

the minimum is over nonnegative a_0, \dots, a_m and b_0, \dots, b_m , and the constraints are

$$a_u + a_{m-v} + b_{u+v} + b_{u-v} \geq 1 \quad (0 \leq v \leq u, u + v \leq m).$$

2. **Odd side length, thin class.** Let $n = 2m + 1$ and consider the thin class C_1 . Then

$$L_{\text{mono}}(2m + 1, 1) = \min \Phi_m^{\text{thin}}(a, b),$$

where

$$\Phi_m^{\text{thin}}(a, b) := 8 \sum_{i=0}^{m-1} a_i + 8 \sum_{i=0}^{m-1} b_i + 4b_m,$$

the minimum is over nonnegative a_0, \dots, a_{m-1} and b_0, \dots, b_m , and the constraints are

$$a_u + a_{m-v-1} + b_{u+v+1} + b_{u-v} \geq 1 \quad (0 \leq v \leq u, u + v \leq m - 1).$$

3. **Even side length.** Let $n = 2m$ and fix either colour class, say C_0 . Then

$$L_{\text{mono}}(2m, 0) = \min \Phi_m^{\text{even}}(a, b, c),$$

where

$$\Phi_m^{\text{even}}(a, b, c) := 8 \sum_{i=0}^{m-1} a_i + 4 \sum_{i=0}^{m-1} b_i + 2c_0 + 4 \sum_{j=1}^{m-1} c_j,$$

the minimum is over nonnegative a_0, \dots, a_{m-1} , b_0, \dots, b_{m-1} and c_0, \dots, c_{m-1} , and the constraints are

$$a_{u-v} + a_{\min(u+v, 2m-1-u-v)} + b_u + c_v \geq 1 \quad (0 \leq v \leq u \leq m-1).$$

The other parity class has the same optimum by reflection.

Proof. The proof is just orbit averaging in the dual. The objective and constraints of the generic dual in Proposition 2 are invariant under every symmetry of the square that preserves the chosen colour class and the four permitted line families. Averaging a feasible dual weighting over this symmetry group keeps it feasible and leaves the objective unchanged. Hence an optimum can be chosen constant on line orbits. Conversely, any feasible reduced weighting defines a feasible weighting for the original dual by assigning the displayed value to every line in the corresponding orbit. Thus the reduced and unreduced optima agree.

For the odd-fat case, the full dihedral group D_4 preserves C_0 . Using the folded coordinates

$$(x, y) = (u + v, u - v), \quad 0 \leq v \leq u, \quad u + v \leq m,$$

every point of the fat class has a representative in this triangle. The two slope- ± 1 diagonal families form one orbit type, represented by a_0, \dots, a_m , and the row/column families form a second, represented by b_0, \dots, b_m . The point represented by (u, v) is covered by the four orbit weights

$$a_u, \quad a_{m-v}, \quad b_{u+v}, \quad b_{u-v},$$

which gives the displayed constraint. The coefficient of each variable in the reduced objective is twice the size of the corresponding line orbit, because the generic dual objective has the prefactor 2. Thus the noncentral orbits have coefficient 8 and the central orbits have coefficient 4. For example, when $n = 7$ and $(u, v) = (2, 1)$, the representative point is $(x, y) = (3, 1)$, and the constraint reads $a_2 + a_2 + b_3 + b_1 \geq 1$.

For the odd-thin class the same averaging group is available, but the fundamental representatives are shifted by half a layer:

$$(x, y) = (u + v + 1, u - v), \quad 0 \leq v \leq u, \quad u + v \leq m - 1.$$

This accounts for the indices $m - v - 1$ and $u + v + 1$ in the constraint. There is no central diagonal orbit of the same type as in the fat case, so the a -sequence has length m , while the row/column sequence still contains the central term b_m with orbit coefficient 4.

For even side length, a quarter-turn swaps the two colour classes, so the averaging group is smaller. In the coordinates

$$u = \frac{x + y}{2}, \quad v = \frac{y - x}{2},$$

a fixed colour class becomes the integer diamond

$$0 \leq u \leq 2m - 1, \quad |v| \leq \min(u, 2m - 1 - u).$$

After folding by the residual colour-preserving symmetries, one may take $0 \leq v \leq u \leq m - 1$. The two oblique line families remain in one orbit type, represented by a_0, \dots, a_{m-1} . The u - and v -families remain distinct and are represented by b_0, \dots, b_{m-1} and c_0, \dots, c_{m-1} . This gives the constraint

$$a_{u-v} + a_{\min(u+v, 2m-1-u-v)} + b_u + c_v \geq 1.$$

Again the objective coefficients are twice the corresponding line-orbit sizes, giving coefficients 8, 4, and 2 exactly as displayed. \square

Table 2: Numerical evidence for the odd-fat reduced LP. Here $n = 2m + 1$ and the comparison value is the continuum certificate value α .

m	n	L_m^{fat}/n	$(L_m^{\text{fat}}/n) - \alpha$
40	81	1.576420575749053	-0.000402821124755
80	161	1.576808190150374	-0.000015206723434
120	241	1.576771111476259	-0.000052285397549
160	321	1.576820185861457	-0.000003211012351

The proposition is a structural compression of the dual. It has the same optimum as the original four-direction dual. Its value is that it exposes the one-dimensional profile structure seen in the computed optima; this profile structure is empirical evidence, not an additional theorem. In the odd-fat case the finite optimal profiles show, on observed active ranges, the interior curvature relation

$$\Delta^2 a_i + 2 \Delta^2 b_j \approx 0,$$

suggested by second-differencing tight constraints in the active region. Representative second-difference data are recorded in Appendix B. Computations in the thin and even cases show similar profile patterns, with the shifted indexing in the thin case and the extra c -profile in the even case.

The computed reduced LPs are consistent with the same candidate limiting slope. Table 2 shows regenerated odd-fat values at larger sizes. These values are already very close to the continuum certificate value α . Like the finite exact-search and LP values in Table 1, these computations are used as motivation and are not part of the companion certificate package.

Complementary computations in the thin and even cases give a similar numerical picture. For example, at sizes around $n \approx 160$ one finds

$$\frac{L_{\text{mono}}(160, 0)}{160} \approx 1.576757, \quad \frac{L_{\text{mono}}(161, 0)}{161} \approx 1.576808, \quad \frac{L_{\text{mono}}(161, 1)}{161} \approx 1.576704.$$

Thus the reduced LP computations suggest a common limiting ratio with candidate value α . The continuum computation in the next subsection supplies an exact upper-bound certificate at this candidate value. With this value of α , the finite computations motivate two related conjectures, which are deliberately separated by strength.

Conjecture 1 (Four-direction LP asymptotics). *Let α be the middle real root of*

$$401\alpha^3 - 1744\alpha^2 + 2240\alpha - 768 = 0.$$

For odd $n = 2m + 1$, let L_m^{fat} and L_m^{thin} denote the relaxation optima on the fat and thin colour classes, respectively. For even $n = 2m$, let L_m^{even} denote the relaxation optimum on either colour class. Then the three symmetry types have the common limiting ratio

$$\lim_{m \rightarrow \infty} \frac{L_m^{\text{fat}}}{2m + 1} = \lim_{m \rightarrow \infty} \frac{L_m^{\text{thin}}}{2m + 1} = \lim_{m \rightarrow \infty} \frac{L_m^{\text{even}}}{2m} = \alpha.$$

Conjecture 2 (Monochromatic NTIL asymptotics). *The exact monochromatic NTIL maxima satisfy*

$$\lim_{n \rightarrow \infty} \frac{D_{\text{mono}}(n)}{n} = \alpha,$$

with the same constant α as in Conjecture 1.

Conjecture 1 is the LP asymptotic suggested by the large finite relaxations. Conjecture 2 is stronger and more speculative: it does not follow from Conjecture 1, because the four-direction

LP is only an upper-bound relaxation of the exact NTIL problem. Exact computation of $D_{\text{mono}}(n, \varepsilon)$ is currently available for the small range shown in Table 1. In the next subsection we prove the continuum statement that supports the constant itself, namely a feasible odd-fat continuum dual pair of objective value α .

4.2 The odd-fat continuum certificate

We now isolate the continuum calculation suggested by the odd-fat reduced dual LP. This subsection gives an explicit feasible dual certificate for the formal continuum problem obtained from the scaled odd-fat reduced dual LP and computes the certificate objective value exactly.

The continuum dual problem

Let $n = 2m + 1$ and consider the fat colour class C_0 . Passing formally, not as a proved continuum-to-discrete limit theorem, to the scaling $u/m \rightarrow x$, $v/m \rightarrow y$, the odd-fat reduced dual program in Proposition 3 leads to the following continuum dual problem. Define

$$\Lambda_{\text{fat}} := \inf 4 \int_0^1 (A(t) + B(t)) dt,$$

where the infimum is over nonnegative functions A, B on $[0, 1]$ satisfying

$$F(x, y) := A(x) + A(1 - y) + B(x + y) + B(x - y) \geq 1$$

on the triangle

$$T := \{(x, y) : 0 \leq y \leq x, x + y \leq 1\}.$$

The theorem below gives an explicit feasible pair (A, B) and hence the upper bound $\Lambda_{\text{fat}} \leq \alpha$.

The certificate

Let p be the real root in the isolating interval

$$\frac{2115883}{10^7} < p < \frac{2115884}{10^7}$$

of

$$401p^3 - 331p^2 + 19p + 7 = 0. \tag{1}$$

Set

$$\begin{aligned} c &= \frac{187p^3 - 211p^2 + 61p - 5}{2(71p^2 - 66p + 11)}, & d &= 1 + p - c, \\ e &= \frac{2c + 3p - 1}{4}, & f &= \frac{-2c + 5p + 1}{4}, & g &= \frac{1 - 3p + 2c}{2}. \end{aligned} \tag{2}$$

For these breakpoints define

$$\begin{aligned} \mathcal{C} &= -c^2 + \frac{1}{2}ce + \frac{1}{2}cf + d^2 - \frac{1}{2}de - \frac{1}{2}df - 2d - g^2 + 2p^2 + 1, \\ \mathcal{D} &= -c - d - 2g + 4p, \\ \mathcal{E} &= -2c^2 + ce + cf - \frac{1}{2}ef - \frac{1}{2}e - \frac{1}{2}f - \frac{1}{2}g^2 + 2p^2, \\ \mathcal{H} &= -2c - g + 4p - 1. \end{aligned}$$

Let K and r be the solution of

$$KC + r\mathcal{D} = 1, \quad K\mathcal{E} + r\mathcal{H} = 1. \tag{3}$$

The exact sign checks recorded in the certificate package give $K > 0$ and $r < 0$. Now put

$$s = -\frac{K}{2}g^2 - rg, \quad \ell = -\left(\frac{K}{2}(e+f) + r\right), \quad q = -\frac{K}{2}ef - \frac{K}{2}g^2 - rg, \quad (4)$$

$$n_1 = Kp^2 + 2rp, \\ \nu = \frac{-2Kc^2 + Kce + Kcf + 2Kp^2 - 2cr + 4pr}{2},$$

and

$$n_2 = \frac{1}{2}(-2Kc^2 + Kce + Kcf + 2Kd^2 - Kde - Kdf - 4Kd \\ + 2Kp^2 - 2cr - 2dr + 4pr).$$

Define the elementary pieces

$$B_Q(t) = \frac{K}{2}t^2 + rt + s, \quad B_L(t) = -\ell t + q, \quad (5)$$

$$A_1(t) = -Kt^2 - 2rt + n_1, \quad A_L(t) = \ell t + \nu, \quad A_2(t) = -Kt^2 + 2Kt + n_2,$$

and finally the two functions

$$A(t) = \begin{cases} 0, & 0 \leq t \leq p, \\ A_1(t), & p \leq t \leq c, \\ A_L(t), & c \leq t \leq d, \\ A_2(t), & d \leq t \leq 1, \end{cases} \quad (6)$$

$$B(t) = \begin{cases} B_Q(t), & 0 \leq t \leq e, \\ B_L(t), & e \leq t \leq f, \\ B_Q(t), & f \leq t \leq g, \\ 0, & g \leq t \leq 1. \end{cases}$$

The two quadratic pieces of B are thus parts of the same parabola. Figure 1 shows the resulting dual profiles on the unit interval.

The verification of the certificate has three parts. First, endpoint and sign inequalities in the cubic field show that the pieces define nonnegative functions A and B on $[0, 1]$; Figure 1 is a visualisation of this certified pair. Second, the obstacle slack

$$G(x, y) = A(x) + A(1 - y) + B(x + y) + B(x - y) - 1$$

is checked on the subdivision shown in Figure 2. On each cell it is quadratic, so nonnegativity follows from the Bernstein coefficient certificate. Finally, direct integration gives the objective value α .

Theorem 1 (Odd-fat continuum dual certificate). *The functions A and B defined in (6) are feasible for the continuum dual problem. Consequently*

$$\Lambda_{\text{fat}} \leq \alpha,$$

where α is the middle real root of

$$401\alpha^3 - 1744\alpha^2 + 2240\alpha - 768 = 0.$$

The formulas above are the certificate used in the proof. Its content is the feasible-pair upper bound for the continuum problem; the discrete asymptotic conjectures remain separate. Appendix C gives the active-patch and stationarity calculation leading to these formulae. The feasibility proof below uses only the displayed definitions and the exact algebraic sign checks.

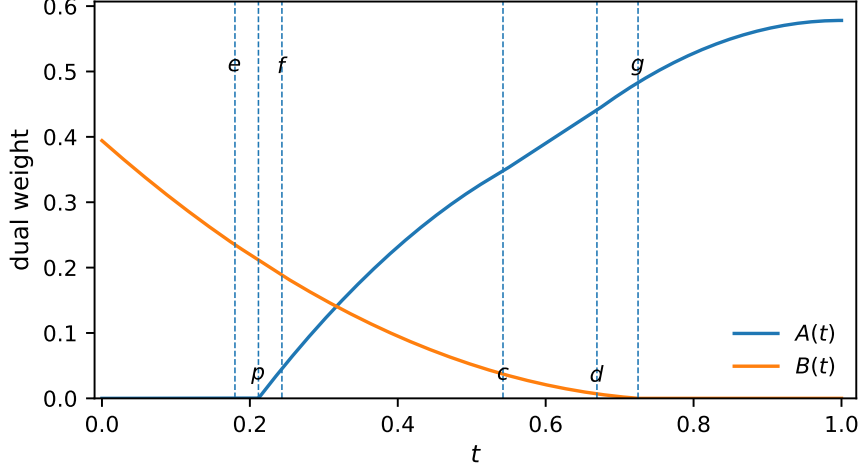


Figure 1: The continuum dual profiles A and B on $[0, 1]$. The zero intervals and the breakpoints p, c, d, e, f, g show the piecewise-profile pattern suggested by the finite dual profiles. The function A is zero up to p , while B vanishes after g ; between the breakpoints the pieces are quadratic or linear as in (6).

Proof of the certificate

Proof of Theorem 1. First, the displayed breakpoints satisfy

$$0 < p < c < d < 1, \quad 0 < e < f < g < 1.$$

Moreover $K > 0$, $r < 0$, and the exact sign checks in the same cubic field give

$$A_1(c) > 0, \quad A_L(d) > 0, \quad A_2(1) > 0,$$

$$B_Q(0) > 0, \quad B_Q(e) = B_L(e) > 0, \quad B_L(f) = B_Q(f) > 0.$$

Since A_1 and A_2 are concave on their intervals, A_L and B_L are linear, and B_Q is convex with zeros at g and $-2r/K - g > g$, these endpoint inequalities prove $A(t), B(t) \geq 0$ on $[0, 1]$.

It remains to prove the obstacle inequality

$$G(x, y) := F(x, y) - 1 \geq 0$$

on T . Put

$$u = x + y, \quad v = x - y.$$

Then

$$x = \frac{u + v}{2}, \quad 1 - y = \frac{2 - u + v}{2},$$

and the triangle T becomes

$$0 \leq v \leq u \leq 1.$$

The breakpoints of the four arguments of A and B cut this triangle by the lines

$$u = e, f, g, \quad v = e, f, g,$$

$$u + v = 2p, 2c, 2d, \quad u - v = 2(1 - d), 2(1 - c),$$

together with the boundary lines $v = 0$, $v = u$ and $u = 1$. The line $u - v = 2(1 - p)$ lies outside the triangle and plays no role. These lines produce 24 nonempty polygonal cells. On each cell, G is a polynomial of degree at most two in (u, v) .

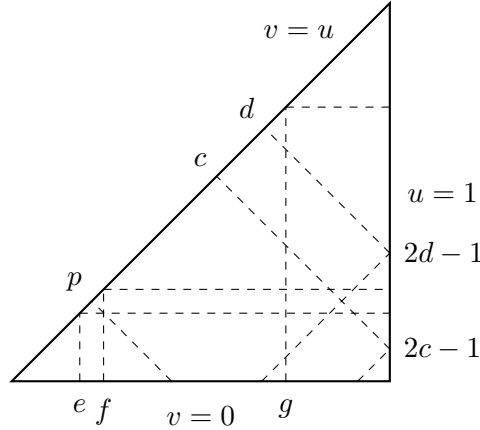


Figure 2: Subdivision of the continuum triangle after the change of variables $u = x + y$ and $v = x - y$, so that T becomes $0 \leq v \leq u \leq 1$. The dashed lines show the breakpoint families $u = e, f, g, v = e, f, g, u + v = 2p, 2c, 2d$, and $u - v = 2(1 - d), 2(1 - c)$ used in the Bernstein-basis obstacle check. The drawing is to scale using decimal approximations of the exact breakpoints.

Triangulate each polygonal cell by a fan from one vertex. This gives 40 triangles. On a triangle with barycentric coordinates $(\lambda_0, \lambda_1, \lambda_2)$, write the quadratic polynomial G in the degree-two Bernstein basis,

$$G = \sum_{i+j+k=2} b_{ijk} \frac{2!}{i!j!k!} \lambda_0^i \lambda_1^j \lambda_2^k.$$

If all Bernstein coefficients b_{ijk} are nonnegative, then G is nonnegative on the whole triangle [15]. For a quadratic these coefficients are obtained from the three vertex values and the three edge-midpoint values.

$$b_{200} = G(V_0), \quad b_{020} = G(V_1), \quad b_{002} = G(V_2),$$

and, for example,

$$b_{110} = 2G\left(\frac{V_0 + V_1}{2}\right) - \frac{G(V_0) + G(V_1)}{2},$$

with the analogous formulae for b_{101} and b_{011} .

All vertices of the 40 triangles have coordinates in $\mathbb{Q}(p)$, where p is the root specified in (1). Hence all Bernstein coefficients lie in the same cubic field. Reducing the 240 coefficients modulo the cubic gives 102 identically zero coefficients and 138 nonzero coefficients. The file `bernstein_coefficients.tsv` in the companion certificate package records each coefficient as

$$c_0 + c_1 p + c_2 p^2 \quad (c_i \in \mathbb{Q}).$$

A Sturm-sequence computation [5] isolates the required root in

$$\frac{2115883}{10^7} < p < \frac{2115884}{10^7}.$$

On this interval, exact rational interval evaluation shows that all 138 nonzero coefficients are positive. Thus every Bernstein coefficient is nonnegative on every triangle in the decomposition, and therefore $G \geq 0$ on T .

Direct integration of the functions in (6), followed by reduction in $\mathbb{Q}(p)$, gives the objective value $4 \int_0^1 (A(t) + B(t)) dt = \alpha$; the algebraic derivation of this identity is recorded in Appendix C. Therefore $\Lambda_{\text{fat}} \leq \alpha$, as claimed. \square

Theorem 1 proves the continuum upper bound $\Lambda_{\text{fat}} \leq \alpha$. Together with the reduced finite LP data, it makes α a plausible candidate for Conjecture 1. A proof of the discrete LP asymptotic would require a continuum-to-discrete approximation theorem, or an independent family of finite dual certificates with objective $\alpha n + o(n)$. Relating the LP asymptotic to the exact monochromatic NTIL optimum remains a separate problem.

A Boundary-forcing heuristic

This appendix records the local forcing argument mentioned in Remark 2. It is included to orient the expected sharpened bound, not as a proof of that bound. The main LP and continuum results are independent of this heuristic forcing argument.

Attaining the diagonal-capacity bound $2n - 2$ would force every relevant diagonal in one slope family to be saturated. Suppose, for example, that the saturated family is the family of slope +1 diagonals and that the two outer singleton diagonals are the opposite corners $(0, n - 1)$ and $(n - 1, 0)$. The other orientation is obtained by reflection.

The two occupied corners already fill the slope-1 diagonal $x + y = n - 1$. Hence the midpoint of the neighbouring length-three diagonal is forbidden, so saturation forces the two endpoints $(0, n - 3)$ and $(2, n - 1)$. The same argument from the opposite corner forces $(n - 3, 0)$ and $(n - 1, 2)$. These new endpoints fill the slope-1 diagonals $x + y = n - 3$ and $x + y = n + 1$. On the next slope-1 diagonal, all three interior points are now forbidden by these three full slope-1 diagonals, so saturation forces the two endpoints $(0, n - 5)$ and $(4, n - 1)$. This creates three points in the top row, a contradiction.

The case in which the outer diagonals have length two is the same local picture with the first step shifted by half a layer. This is the heuristic reason to expect that $2n - 2$ points are impossible for $n \geq 6$.

For $2n - 3$ points there is exactly one unit of missing capacity in each diagonal family. If the defect in a chosen slope family lies away from the first few boundary diagonals used above, the same forcing chain runs unchanged. If both defects are boundary defects, the two slope families affect different pairs of corners, so at least one corner still supports an unbroken forcing chain. Starting there again forces three points in a row or column. This is the heuristic reason to expect that $2n - 3$ points are impossible as well.

B Finite odd-fat profile curvature data

This appendix records the finite-profile data referred to in Subsection 4.1. The data are not used in the proof of Theorem 1. They document one observed interior curvature pattern that motivated the piecewise quadratic-linear certificate.

Table 3: Second-difference evidence for the odd-fat reduced dual profiles. The windows are interior active ranges of the finite optimal profiles. The displayed averages are scaled by m^2 .

m	a window	$m^2 \text{ avg } \Delta^2 a$	b window	$m^2 \text{ avg } \Delta^2 b$	$\Delta^2 a / \Delta^2 b$
40	30...38	-2.4794669146	15...22	1.2397334573	-2.0000000000
80	60...78	-2.5053826581	30...44	1.2526913290	-2.0000000000
120	90...118	-2.4811188008	45...66	1.2405594004	-2.0000000000
160	120...158	-2.4686298381	60...88	1.2343149191	-2.0000000000

C Derivation of the odd-fat continuum certificate

This appendix records the symbolic ansatz calculation that produced the breakpoints and coefficients used in the continuum certificate of Subsection 4.2. The proof of Theorem 1 uses the resulting functions directly; the calculation below explains how the active pieces were found.

The finite odd-fat LP profiles motivate the piecewise structure displayed in (6). The function A is zero near the lower endpoint, then quadratic, linear, and quadratic again, while B is quadratic, linear, quadratic, and then zero. Continuity and the endpoint conditions force the coefficient relations in (4). In particular,

$$\nu = A_1(c) - \ell c, \quad n_2 = A_L(d) + Kd^2 - 2Kd.$$

The quadratic active patch

$$A_1(x) + A_2(1 - y) + B_Q(x + y) + B_Q(x - y) = 1$$

contributes the scalar equation

$$Q := n_1 + n_2 + K + 2s - 1 = 0.$$

The linear active patch

$$A_L(x) + A_L(1 - y) + B_L(x - y) = 1$$

contributes

$$R := \ell + 2\nu + q - 1 = 0.$$

After substituting the coefficient relations, these two equations take the linear form

$$Q = KC + r\mathcal{D} - 1, \quad R = K\mathcal{E} + r\mathcal{H} - 1,$$

where $\mathcal{C}, \mathcal{D}, \mathcal{E}, \mathcal{H}$ are the expressions defined in the certificate. Thus (3) is exactly the condition $Q = R = 0$.

The objective value of the piecewise pair is

$$\begin{aligned} \Phi = 4 \left(\int_p^c A_1(t) dt + \int_c^d A_L(t) dt + \int_d^1 A_2(t) dt \right. \\ \left. + \int_0^e B_Q(t) dt + \int_e^f B_L(t) dt + \int_f^g B_Q(t) dt \right). \end{aligned}$$

Performing the integrations and substituting the coefficient relations gives

$$\Phi = K\mathcal{A} + r\mathcal{B},$$

where

$$\begin{aligned} \mathcal{A} = \frac{8}{3}c^3 - c^2e - c^2f - 4c^2 + 2ce + 2cf - \frac{8}{3}d^3 + d^2e + d^2f + 8d^2 \\ - 2de - 2df - 8d - \frac{1}{3}e^3 + e^2f - ef^2 + \frac{1}{3}f^3 - \frac{4}{3}g^3 - \frac{8}{3}p^3 + 4p^2 + \frac{8}{3}, \end{aligned}$$

and

$$\mathcal{B} = 2c^2 - 4c + 2d^2 - 4d - 2g^2 - 4p^2 + 8p.$$

Introducing Lagrange multipliers λ, μ for the two constraints $Q = R = 0$, the stationarity equations for

$$\mathcal{L} = \Phi + \lambda Q + \mu R$$

are

$$Q = 0, \quad R = 0,$$

$$\begin{aligned}
\mathcal{A} + \lambda\mathcal{C} + \mu\mathcal{E} &= 0, & \mathcal{B} + \lambda\mathcal{D} + \mu\mathcal{H} &= 0, \\
(Kp + r)(2p - 2 - \lambda - \mu) &= 0, \\
(4c - \lambda - 2\mu - 4)(4Kc - Ke - Kf + 2r) &= 0, \\
(4d - \lambda - 4)(-4Kd + Ke + Kf + 4K + 2r) &= 0, \\
0 = 2c^2 - c\lambda - 2c\mu - 4c - 2d^2 + d\lambda + 4d \\
&\quad + 2e^2 - 4ef + 2f^2 + f\mu + \mu, \\
0 = 2c^2 - c\lambda - 2c\mu - 4c - 2d^2 + d\lambda + 4d \\
&\quad - 2e^2 + 4ef + e\mu - e - 2f^2 + \mu,
\end{aligned}$$

and

$$(Kg + r)(4g + 2\lambda + \mu) = 0.$$

The branch used in the certificate is the nondegenerate branch

$$\lambda + \mu = 2p - 2, \quad \lambda + 2\mu = 4c - 4, \quad \lambda = 4d - 4, \quad 2\lambda + \mu = -4g.$$

Equivalently,

$$d = 1 + p - c, \quad g = \frac{1 - 3p + 2c}{2}, \quad \lambda = 4(p - c), \quad \mu = 4c - 2p - 2.$$

On this branch, adding and subtracting the two equations obtained by varying e and f gives

$$(2p - e - f)(-2c + p + 1) = 0,$$

and

$$(e - f)(-2c + 2e - 2f + p + 1) = 0.$$

The branch matching the certified breakpoint ordering is therefore

$$e + f = 2p, \quad f - e = \frac{1 + p - 2c}{2},$$

which gives the formulae for e and f used in the certificate.

It remains to solve for p and c . Substituting these branch relations into the stationarity equations for r and K gives

$$-4c^2 - 4cp + 4c + 13p^2 - 10p + 1 = 0,$$

and

$$88c^3 - 36c^2p - 36c^2 - 126cp^2 + 132cp - 30c + 29p^3 - 57p^2 + 39p - 3 = 0.$$

Eliminating c gives

$$(p - 1)^2(5p - 1)(401p^3 - 331p^2 + 19p + 7) = 0.$$

The ordering constraints single out the middle real root of (1). Substitution into the objective and exact reduction in $\mathbb{Q}(p)$ gives

$$\Phi = \alpha,$$

where eliminating p yields

$$401\alpha^3 - 1744\alpha^2 + 2240\alpha - 768 = 0,$$

and the root compatible with the numerical value of the integral is the middle real root.

Computational reproducibility and certificate package

The continuum feasibility part of Theorem 1 is a finite exact algebraic check in the cubic field $\mathbb{Q}(p)$. The companion directory `odd_fat_certificate/` contains `README.md`, `constants.tsv`, `sign_checks.tsv`, `triangles.tsv`, `bernstein_coefficients.tsv`, and `verify_odd_fat_certificate.py`. These files record the exact constants, the exact sign checks, the triangulation of the continuum domain, and the exact Bernstein coefficients for the obstacle polynomial on each triangle. The verification script regenerates the certificate and uses exact rational arithmetic for the algebraic sign checks; it requires Python 3 and `shapely` for the subdivision step. The check is run from within `odd_fat_certificate/` by executing `python verify_odd_fat_certificate.py`. In the regenerated certificate the 240 Bernstein coefficients split into 102 identically zero coefficients and 138 positive coefficients, all represented as elements of $\mathbb{Q}(p)$. The package verifies the continuum obstacle certificate; it does not certify the finite LP values in Tables 1 and 2, the exact NTIL search data, or the continuum-to-discrete conjectures. The exact value of the integral is the symbolic calculation recorded in Appendix C.

Declaration of generative AI and AI-assisted technologies

During the preparation of this manuscript the author used OpenAI ChatGPT to assist with editorial checks and L^AT_EX organisation. The mathematical content was reviewed and edited by the author, who takes full responsibility for the final version.

References

- [1] M.A. Adena, D.A. Holton, P.A. Kelly, Some thoughts on the no-three-in-line problem, in: D.A. Holton (ed.), *Combinatorial Mathematics: Proceedings of the Second Australian Conference*, Lecture Notes in Mathematics 403, Springer, Berlin, 1974, pp. 6–17. doi:10.1007/BFb0057371.
- [2] O. Aichholzer, D. Eppstein, E.-M. Hainzl, Geometric dominating sets—a minimum version of the No-Three-In-Line Problem, *Comput. Geom.* 108 (2023), Article 101913. doi:10.1016/j.comgeo.2022.101913.
- [3] D.B. Anderson, Update on the no-three-in-line problem, *J. Combin. Theory Ser. A* 27 (1979) 365–366. doi:10.1016/0097-3165(79)90025-6.
- [4] J. Balogh, F.C. Clemen, A. Dumitrescu, D. Liu, Subset selection problems in planar point sets, arXiv:2412.14287 (2024).
- [5] S. Basu, R. Pollack, M.-F. Roy, *Algorithms in Real Algebraic Geometry*, 2nd ed., Springer, Berlin, 2006. doi:10.1007/3-540-33099-2.
- [6] P. Brass, W.O.J. Moser, J. Pach, *Research Problems in Discrete Geometry*, Springer, New York, 2005. doi:10.1007/0-387-29929-7.
- [7] C. Cao, Study on Two Optimization Problems: Line Cover and Maximum Genus Embedding, Master’s thesis, Texas A&M University, May 2012. <https://hdl.handle.net/1969.1/ETD-TAMU-2012-05-11073>.
- [8] Ullas Chandran S.V., G. Di Stefano, Haritha S., E.J. Thomas, J. Tuite, Colouring a graph with position sets, *Ars Math. Contemp.*, early access (2025). doi:10.26493/1855-3974.3454.a3c.

- [9] A.S. Cooper, O. Pikhurko, J.R. Schmitt, G.S. Warrington, Martin Gardner’s minimum no-3-in-a-line problem, *Amer. Math. Monthly* 121 (2014) 213–221. doi:10.4169/amer.math.monthly.121.03.213.
- [10] J. Cooper, J. Hyatt, Permutations minimizing the number of collinear triples, *Des. Codes Cryptogr.* 93 (2025) 3135–3142. doi:10.1007/s10623-025-01632-w.
- [11] J.N. Cooper, J. Solymosi, Collinear points in permutations, *Ann. Comb.* 9 (2005) 169–175. doi:10.1007/s00026-005-0248-4.
- [12] H. Dudeney, *Amusements in Mathematics*, Nelson, Edinburgh, 1917.
- [13] A. Dumitrescu, General Position Subset Selection in Line Arrangements, *Algorithms* 18 (2025), 315. doi:10.3390/a18060315.
- [14] D. Eppstein, *Forbidden Configurations in Discrete Geometry*, Cambridge University Press, Cambridge, 2018. doi:10.1017/9781108539180.
- [15] R.T. Farouki, The Bernstein polynomial basis, a centennial retrospective, *Comput. Aided Geom. Design* 29 (2012) 379–419. doi:10.1016/j.cagd.2012.03.001.
- [16] A. Flammenkamp, Progress in the no-three-in-line problem, *J. Combin. Theory Ser. A* 60 (1992) 305–311.
- [17] A. Flammenkamp, Progress in the No-Three-in-Line Problem, II, *J. Combin. Theory Ser. A* 81 (1998) 108–113.
- [18] J. Fowler, A. Groot, D. Pandya, B. Snapp, The no-three-in-line problem on a torus, *arXiv:1203.6604* (2012).
- [19] V. Froese, I. Kanj, A. Nichterlein, R. Niedermeier, Finding points in general position, *Int. J. Comput. Geom. Appl.* 27 (2017) 277–296. doi:10.1142/S021819591750008X.
- [20] Z. Füredi, Maximal independent subsets in Steiner systems and in planar sets, *SIAM J. Discrete Math.* 4 (1991) 196–199. doi:10.1137/0404019.
- [21] R.K. Guy, P.A. Kelly, The no-three-in-line problem, *Canadian Math. Bull.* 11 (1968) 527–531.
- [22] R.R. Hall, T.H. Jackson, A. Sudbery, K. Wild, Some advances in the no-three-in-line problem, *J. Combin. Theory Ser. A* 18 (1975) 336–341. doi:10.1016/0097-3165(75)90043-6.
- [23] H. Harborth, P. Oertel, T. Prellberg, No-three-in-line for seventeen and nineteen, *Discrete Math.* 73 (1988/89) 89–90.
- [24] T. Kløve, On the No-Three-in-Line Problem, III, *J. Combin. Theory Ser. A* 26 (1979) 82–83. (See also related notes in the same volume.)
- [25] B. Kovács, Z.L. Nagy, D.R. Szabó, Randomised algebraic constructions for the no- $(k + 1)$ -in-line problem, *arXiv:2508.07632* (2025).
- [26] C.Y. Ku, K.B. Wong, On No-Three-In-Line Problem on m -Dimensional Torus, *Graphs Combin.* 34 (2018) 355–364. doi:10.1007/s00373-018-1878-8.
- [27] D.T. Nagy, Z.L. Nagy, R. Woodroffe, The extensible No-Three-In-Line problem, *European J. Combin.* 114 (2023), Article 103796. doi:10.1016/j.ejc.2023.103796.
- [28] M.S. Payne, D.R. Wood, On the general position subset selection problem, *SIAM J. Discrete Math.* 27 (2013) 1727–1733. doi:10.1137/120897493.

- [29] A. Pór, D.R. Wood, No-three-in-line-in-3D, *Algorithmica* 47 (2007) 481–488. doi:10.1007/s00453-006-0158-9.
- [30] T. Prellberg, Constraint satisfaction programming for the no-three-in-line problem, arXiv:2602.07751 (2026).
- [31] A. Schrijver, *Theory of Linear and Integer Programming*, Wiley, Chichester, 1998. ISBN 978-0-471-98232-6.
- [32] M. Skotnica, No-three-in-line problem on a torus: periodicity, *Discrete Math.* 342 (2019) 111611. doi:10.1016/j.disc.2019.111611.
- [33] D.R. Wood, A note on colouring the plane grid, *Geombinatorics* XIII(4) (2004) 193–196. <https://users.monash.edu.au/~davidwo/papers/Wood-GridColouring.pdf>.